3441

Optimal Synthesis of Multicomponent Zeotropic Distillation Processes. 2. Preprocessing Phase and Rigorous Optimization of Efficient Sequences

Mariana Barttfeld and Pío A. Aguirre*

INGAR, Instituto de Desarrollo y Diseño, Universidad Nacional del Litoral, Avellaneda 3657, (3000) Santa Fe, Argentina

The optimal synthesis of zeotropic efficient distillation processes is addressed in this paper. The reversible distillation sequence model (RDSM) is rigorously approximated by a sequence of adiabatic units. Alternative superstructures representations involving different energy distributions are proposed for approximating the RDSM. The efficient distillation synthesis problem is formulated as a rigorous tray-by-tray mixed-integer nonlinear programming (MINLP) problem. Discrete decisions are related to the feed and heat-exchange locations while continuous choices select the operating conditions of the process. The most suitable representation is selected by computing the entropy production of each scheme. The solution procedure includes an automatic preprocessing phase where reversible distillation theory is combined with mathematical programming to generate initial values and bounds for the variables involved in the rigorous MINLP problem. Convergence and robustness of the formulations are considerably improved by including this preliminary phase. Numerical examples are reported for the separation of zeotropic mixtures to show the performance of the proposed methodology.

1. Introduction

The synthesis of a process addresses the fundamental problem of structuring a proper scheme to satisfy certain goals. The separation of more than two components by continuous distillation has been accomplished by arranging columns in series. Several conventional alternative configurations exist, most notably, the conventional indirect (direct) sequences where the least (most) volatile component is completely removed first.

Basically, two different kinds of distillation sequences were proposed in the literature: conventional and complex arrangements. In the last one, lower thermal energy use is required by coupling the units.

It is well-established that the employment of complex columns configurations leads to significant savings of both capital and energy costs. However, there are two major difficulties associated with the design of these schemes. First, the number of design variables is notably increased by additional degrees of freedom related to the column interconnection streams. The mathematical formulations exhibit significant computational difficulties and they largely depend on good initial values and tight bounds for the state variables.[1] Disjunctive mathematical formulations have shown to overcome some of these limitations; however, bounding and initializing variables remain main issues for the success of computational demand of the approach.[2,3] Second, the large number of design alternatives increases tremendously when complex columns are considered as potential alternatives.

In a previous work, we observed that the use of a good initial guess enhances the convergence and robustness of the single-column synthesis problem.[4] In the synthesis of complex columns, due to the complexity and large number of degrees of freedom that the formulations involve, the use of good initial solutions and bounds are even more helpful to lead the solutions to feasible designs.

The objective of this work is then to develop a procedure to obtain a good initial solution for the synthesis problem of complex distillation processes. An efficient solution is a feasible solution for the economic problem. The major objective of this paper is to present a methodology for the synthesis of complex efficient zeotropic multicomponent distillation sequences. A superstructure based on the reversible distillation sequence model (RDSM)[5] is proposed, which encloses conventional and complex designs as well.[6] The reversible separation task[5,7] is selected to be performed in each single adiabatic column of the scheme. Even though the separation task is specified, the optimal energy distribution for approximating the RDS (reversible distillation sequence) is a degree of freedom of the model. Three different scenarios involving different energy distributions will be studied by specifying proper interconnection stream compositions and flow rates to derive the most efficient arrangement of columns.

The complete synthesis procedure involves a preprocessing phase with well-behaved NLP problems. The formulations are successively solved and no external information or turning parameters have to be used. No simplifying assumptions are needed on physical-chemical properties and material and energy balances.

This paper is organized as follows. In the next section the problem is stated. We examine in section 3 the superstructure for the efficient synthesis sequence problem. In section 4, the different efficient scenarios are studied and in section 5, the mathematical models for the preprocessing phase and for the rigorous MINLP problem are presented. In section 6, solution procedures

---

* To whom correspondence should be addressed. Fax: 0342-4553439. E-mail: paguir@ceride.gov.ar.
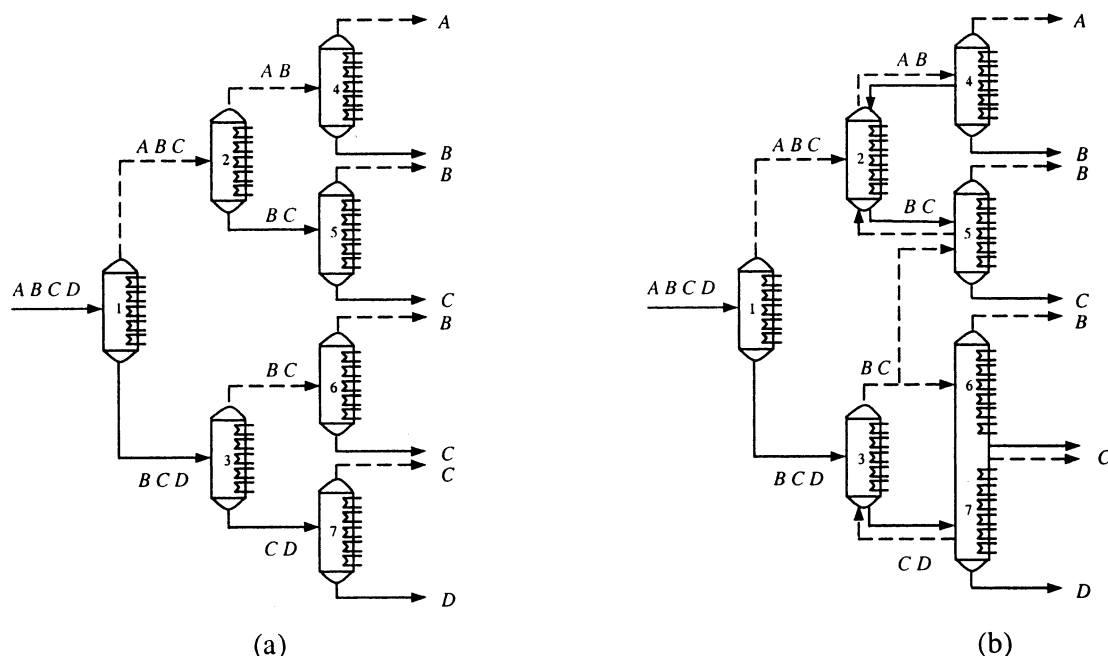
Figure 1. RDSM for a four-component mixture.

are proposed and in section 7, numeric examples are presented. Finally, the conclusions of this work are outlined.

2. Problem Statement

The problem can be stated as follows. Given is the composition, flow rate, and thermal state of a multi-component zeotropic feed with NC components. The problem consists of synthesizing an efficient distillation process involving maximum efficiency and low-energy demand to produce NC pure products.

3. Efficient Distillation Superstructure

According to Kaibel et al.,[8] for the development of an efficient distillation process the following points should be considered: (1) intermediate reboilers and condensers; (2) a sufficient number of theoretical stages in each column; (3) a small pressure drop; (4) as far as possible direct heat and mass transfer to avoid heat exchangers; (5) an appropriated enthalpy for the feed; (6) the correct thermodynamic separation sequence.

On the basis of these characteristics, a general separation scheme can be derived where the reversible separation task takes place in each column. In Figure 1a, the RDS is shown for a four-component zeotropic feed. This sequence has seven columns arranged in three levels. Note that the number of units to achieve essentially pure components as well as the number of levels of the sequence can be expressed in terms of the number of components NC and the feed, respectively: $2^{NC-1} - 1$ and $NC - 1$.[6]

The RDS sequence can be rearranged in various ways. Top products can be specified as boiling liquids or saturated vapors. Some liquid reflux and vapor reboil can be taken directly from the following unit. In Figure 1b, the side liquid product of column 4 provides part of the reflux of column 2. The units can be combined if the liquid and vapor streams at the connection point have the same temperature and composition. Note that, in the RDS, only sections from where pure products

emerge can be combined. In Figure 1b, the stripping section of column 6 and the rectifying section of column 7 can be joined since pure product C emerges from both. Furthermore, binary mixtures of the same components but different composition can be fed to one single column and column triplets can be combined to a single unit with a vertical partition.[6]

In each column of the reversible sequence, the reversible[5] or preferred[7] separation task is performed. For any given multicomponent zeotropic mixtures, the reversible separation mass-balance line coincides with the feed equilibrium vector, which can be computed with the liquid and vapor feed compositions.

Each column of the reversible sequence can be approached by an adiabatic unit.[9] If reversibility conditions are relaxed, the RDS can be approximated by the RD-based sequence (RDS-based). Each column still performs the reversible nonsharp separation but the energy is not continuously distributed in each unit. Only one heat exchanger is placed at each column extreme. This fact changes neither the product compositions nor the column overall energy demands but it affects the column internal composition profiles and the external heating and cooling levels.

In Figure 2, the RDS-based superstructure approximation for the sequence of Figure 1 is shown. The heat is exchanged at each column extreme instead of being continuously distributed along the unit (see Figure 1). The units are directly coupled to allow mass and energy integration between them. For simplicity, two different zones are considered in the superstructure according to the type of integration that takes place. Zone A (see Figure 2) includes columns fed by multicomponent mixtures. The units are interconnected by liquid and vapor streams, which provide part of the reboil or reflux to the columns, respectively. To avoid entropy production in the system, the vapor and liquid steams interconnecting one unit with a previous one are in equilibrium. Zone B (see Figure 2) includes those units that are fed by binary mixtures or from where pure products emerge. These columns are located in the last level of
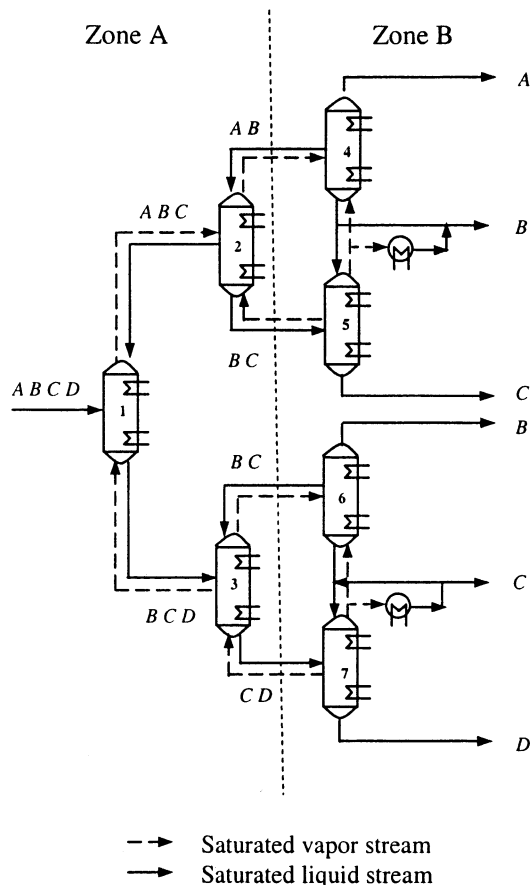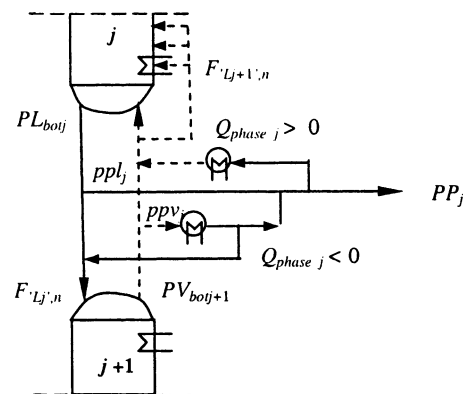
Figure 2. General RDS-based superstructure for a four-component mixture.

Figure 3. Superstructure for the heat integration in zone B.

the superstructure. Sections from where the same pure product emerges can be combined. To illustrate this point, consider the integration between column 4 and column 5 in Figure 2. Note that the superstructure involves a reboiler in column 4 bottom and a condenser in column 5 top. Since these two sections can be combined, the energy exchanged in both sections can be integrated. Let us assume that the amount of energy demanded in the reboiler of column 4 is smaller than the energy required in the condenser of column 5. Then, part of the energy that column 5 needs to reject can be used to produce the vapor flow originally produced by the reboiler of column 4. As the result of the integration, column 4 will not have a reboiler. The opposite situation takes place when the energy rejected in the condenser of column 5 is not enough to produce the necessary vapor reboiler for column 4. Then a reboiler has to be placed in column 4 bottom and no condenser is needed in the rectifying section of column 5. Note that the stripping section of column 6 can also be integrated with the rectifying section of column 7 since pure C emerges from both.

In Figure 3, the superstructure for the column integration is shown. The product flow emerging from the integrated sections, PP_j, can be formed by the contribution of the liquid product of column j, ppl_j, as well as from the contribution of the vapor product of column $j + 1$, ppv_j. The superstructure involves the energy $Q_{\text{phase}j}$ to convert the remaining liquid in vapor flows and vice versa. Note that, for modeling variable reboiler location, the secondary feed $F_{Lf,n}$ has variable location.

It is worth noting that the RDS-based superstructure proposed for the efficient sequence synthesis model includes all conventional and complex schemes. The efficient solution keeps all the elements of the initial superstructure proposed. This fact allows the use of efficient designs as starting points for the economic problem of distillation sequence design. If a cost-based objective function is minimized, some column sections may disappear from the efficient solution. Many alternatives can be derived from the superstructure proposed. Sections with similar column section diameters, compositions, and temperature of the products will allow combining the sections in the final solution, as in the case studied by Aguirre et al.[10]

4. Efficient Scenarios

As was stated in section 2, the specifications for the main feed and final products are given. However, the compositions and flow rates of all the internal streams that interconnect the units are unknown. As the energy involved in each column depends on the products specifications, the energy distribution in the sequence is also unknown. Therefore, the synthesis of an efficient design involves finding the energy distribution of the sequence as well as the total heat loads.

We are interested in closely approximating the RDS by a sequence of adiabatic units, each one with one condenser and one reboiler. Then it has to be determinated which part of the energy required in each column of zone A will be supplied by the columns integration and which part by utilities to perform the separation involving minimum entropy production. Different scenarios involving different energy distribution can be proposed. To characterize a certain scenario, the *extent of the integration* that takes place is defined. The extent of integration of a scenario denotes the amount of energy that is provided by the integration of columns. Then a maximum extent of integration of the sequence means that all the energy involved in the columns located in zone A and zone B (except for the columns located in the extremes of zone B) is supplied by the integration between sections.

The extent of integration in the columns of zone A can be indirectly selected by orienting the product (feeds) composition emerging (entering) from (to) each single unit. Three RDS-based scenarios with different extents of integration are considered in this work. Scenario 1 is a fully thermally coupled scheme (Petlyuk column for ternary mixtures) that involves a maximum extent of integration (see Figure 4a). In this configuration, the heat is exchanged at nonfavorable temperature levels: the complete amount of energy required for the

(a)

(b)

(c)
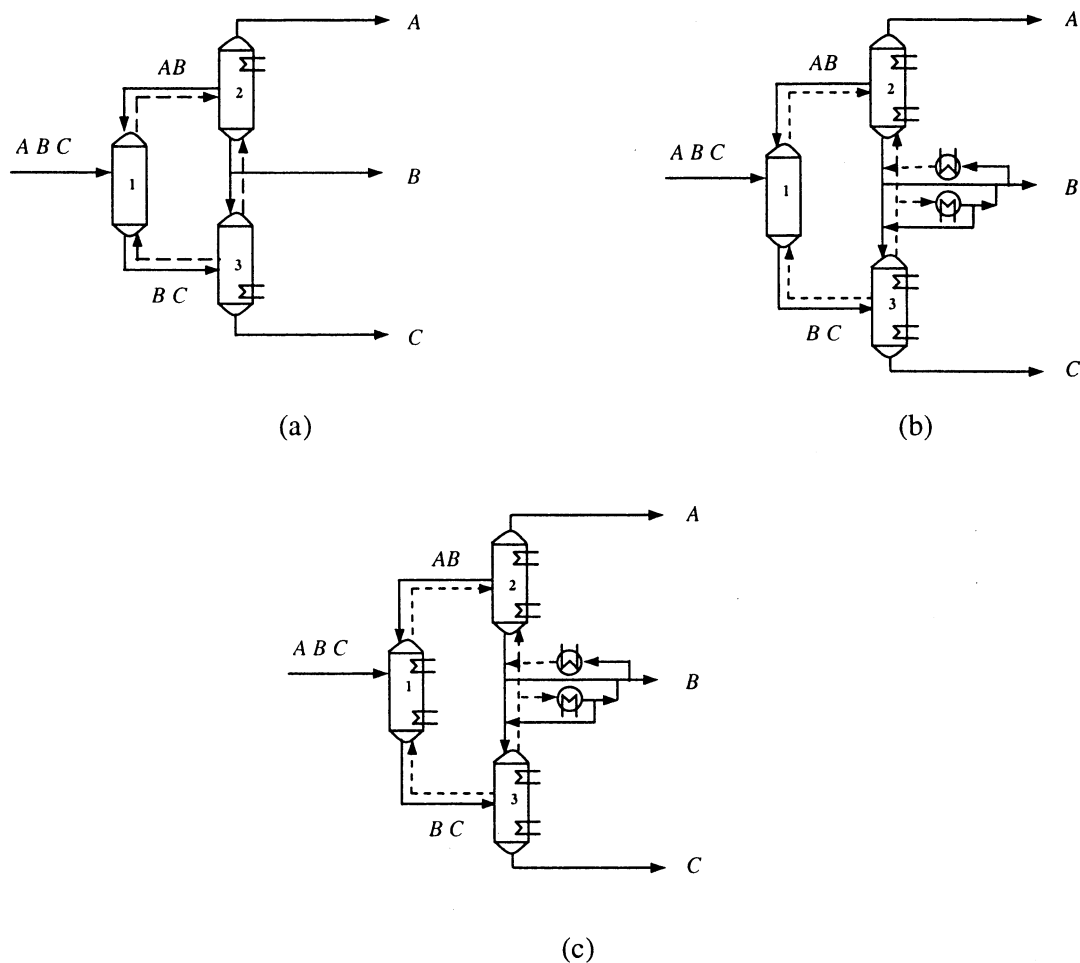
Figure 4. Superstructures for efficient RDS-based scenarios.

separation is rejected at T_A, which is the lowest temperature of the system and added at the highest temperature T_C.

Scenario 2 is a fully thermally coupled scheme with direct integration in zone B (see Figure 4b). In this sequence the heat is exchanged at more favorable temperature levels than scenario 1. Part of the energy is rejected in the column 3 condenser at temperature T_B instead of exchanging the complete amount at T_A. The same holds if the resultant heat after the integration in zone B is exchanged in column 2 reboiler. Instead of adding the complete amount at T_C, a part is exchanged at a lower temperature T_B.

In scenario 3, the extent of integration is lower than the maximum one (see Figure 4c). Consequently, column 1 has a condenser and a reboiler. As in the previous case, the bottom of column 2 is directly integrated with the top of column 3.

In scenarios 1 and 2, column 1 does not involve heat exchange. For that reason, the composition of the interconnecting vapor and liquid streams which provide the reflux and reboil, respectively, will be oriented to have the saddle pinch point composition. Note that a column which approximates a reversible unit does not involve heat exchange between the feed tray and the saddle pinch point regions (see ref 9 for details). In scenario 3, the energy involved in column 1 is determined if the composition and flow of the interconnecting streams are specified. For this scenario, the reversible exhausting pinch point compositions are specified. Note that the reversible exhausting pinch points are the

points of the rectifying (stripping) reversible profile where the heaviest (lightest) component is completely removed (see Appendix A for details).

5. Sequence Model Formulation

In this section, the general formulation for the efficient sequence design is presented. Due to the complexity of the rigorous model, a preprocessing phase is first formulated. The models involved in the preliminary solution phase are presented in section 4.1 while the sequence tray-by-tray rigorous formulation is presented in section 5.2.

5.1. Preprocessing Phase Models. The objective of the preprocessing phase is to compute initial values and bounds for the main variables in the rigorous efficient sequence model.

The preprocessing phase involves two steps. In the first step, the preprocessing phase for each single column[9] is considered. Each single column of the reversible scheme (see Figure 1 for a four-component feed example) is modeled with overall balances to the rectifying and stripping sections. In a second step, the sequence preprocessing phase is considered to compute initial values and bounds related to the interconnecting flows and energy demand considering the columns integration.

It should be noted that all the preprocessing formulations involve overall mass and energy balances; however, the vapor−liquid equilibrium (VLE) is rigorously formulated.
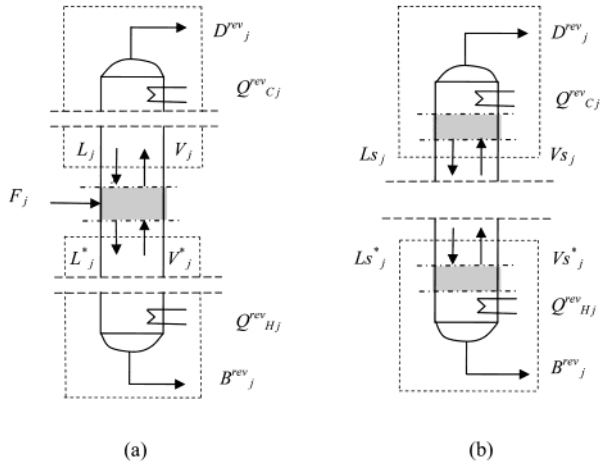
Figure 5. Control volumes for the reversible products and saddle pinch point calculations.

Next, the models involved in the preprocessing phase are presented. Note that a solution procedure for systematically solving these problems is presented in section 6.

Single-Column Preprocessing Phase. Consider the following set definitions. Let NCOL be the set denoting a column j of the RDS-based sequence: $j = 1, 2, ..., J = 2^{NC-1} - 1$. Let C be the set of components i present in the feed: $C = \{i | i = 1, ..., NC\}$. Given is the composition of the feed entering column j. A flash calculation computes the feed vapor and liquid composition $y_{j,i}^F$ and $x_{j,i}^F$, respectively. Given are the feed flow rate F_j and vapor fraction q_j. The reversible distillate and bottom products composition, x_{i,D_j}^{rev} and x_{i,B_j}^{rev}, products flow rates, D_j^{rev} and B_j^{rev}, and condenser and reboiler energy demands, Q_{Cj}^{rev} and Q_{Hj}^{rev}, respectively, can be computed by solving the theoretical reversible model (TRM), which is presented next (see Figure 5a):

TRM:

$$\min z_{TRMj} = x_{h,D_j}^{rev} + x_{l,B_j}^{rev} \quad (1)$$

s.t.

$$\left.\begin{array}{l} L_j + D_j^{rev} = V_j \\ L_j x_{j,i} + D_j^{rev} x_{i,D_j}^{rev} = V_j y_{j,i} \;\forall\, i \in C \\ L_j h_{L_j} + D_j^{rev} h_{D_j} + Q_{Cj}^{rev} = V_j h_{V_j} \end{array}\right\} \forall\, j \in NCOL \quad (2)$$

$$\sum_{i=1}^{NC} x_{i,D_j}^{rev} = 1 \qquad \sum_{i=1}^{NC} y_{i,D_j}^{rev} = 1 \quad (3)$$

$$\left.\begin{array}{l} L_j^* = V_j^* + B_j^{rev} \\ L_j^* x_{j,i} = V_j^* y_{j,i} + B_j^{rev} x_{i,B_j}^{rev} \;\forall\, i \in C \\ L_j^* h_{L_j} + Q_{Hj}^{rev} = V_j^* h_{V_j} + B_j^{rev} h_{B_j} \end{array}\right\} \forall\, j \in NCOL \quad (4)$$

$$\sum_{i=1}^{NC} x_{i,B_j}^{rev} = 1 \qquad \sum_{i=1}^{NC} y_{i,B_j}^{rev} = 1 \quad (5)$$

$$\left.\begin{array}{l} x_{j,i} = x_{j,i}^F \\ y_{j,i} = y_{j,i}^F \end{array}\right\} \forall\, i \in C, j \in NCOL \quad (6)$$

$$\left.\begin{array}{l} L_j + (1 - q_{F_j})F_j = L_j^* \\ V_j + q_{F_j}F_j = V_j^* \end{array}\right\} \forall\, j \in NCOL \quad (7)$$

$$K_{j,i} = K_{j,i}(x_j, y_j, T_j, p) \;\forall\, i \in C, j \in NCOL \quad (8)$$

$$\left.\begin{array}{l} h_{L_j} = h_{L_j}(x_j, T_j, p) \\ h_{V_j} = h_{V_j}(y_j, T_j, p) \end{array}\right\} \forall\, j \in NCOL \quad (9)$$

The objective function of this problem is given by expression (1). The reversible products compositions are calculated by minimizing the composition of the heaviest component in the distillate product x_{h,D_j}^{rev} and the lightest component composition in the bottom product x_{l,B_j}^{rev} emerging from column j. Note that "h" and "l" are the heaviest and lightest components, respectively. The mass balance of the separation is oriented in the reversible direction by imposing constraints in the problem. Equations 2 and 3 are overall balances formulated to a reversible rectifying section operating under minimum reflux conditions (see Figure 5a). Balances for the reversible stripping section are given by eqs 4 and 5. Due to the existence of a double pinch point around the feed tray, the vapor and liquid composition $y_{j,i}$ and $x_{j,i}$ entering and leaving this tray, respectively, are the same as the feed vapor and liquid composition previously calculated in the flash model. This condition is imposed in eq 6. The equations in (7) connect both column sections by formulating liquid and vapor balances in the feed tray. The VLE is assumed ideal and it is modeled by eq 8 and the enthalpies for the liquid and vapor phases are modeled in eq 9. The pressure is assumed constant.

The solution obtained from the model (TRM) is used to compute the saddle pinch points that take place in each adiabatic unit (see ref 9). Overall balances are formulated to a control volume of an adiabatic column j involving each column extreme and the region where the saddle pinch point takes place (see Figure 5b). The vapor and liquid compositions, $ys_{j,i}$ and $xs_{j,i}$, and the flows rate of the vapor and liquid streams entering and leaving the saddle pinch points of a column j, Vs_j and Ls_j, are calculated by solving the saddle pinch point model (SPPM) given by the following system of equations:
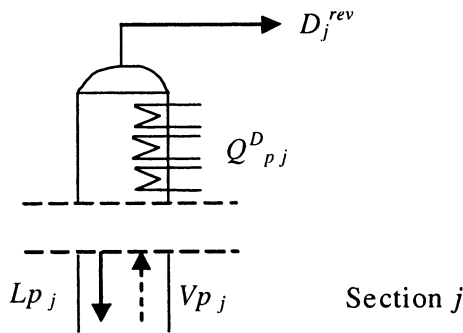
SPPM:

$$\left.\begin{array}{l} Ls_j + D_j^{rev} = Vs_j \\ Ls_j xs_{j,i} + D_j^{rev} x_{i,D_j}^{rev} = Vs_j ys_{j,i} \;\forall\, i \in C \\ Ls_j hs_{L_j} + D_j^{rev} h_{D_j} + Q_{Cj}^{rev} = Vs_j hs_{V_j} \end{array}\right\}$$
$$\forall\, j \in NCOL, j \le 2^{NC-2} - 1 \quad (10)$$

$$\sum_{i=1}^{NC} xs_{j,i} = 1 \qquad \sum_{i=1}^{NC} ys_{j,i} = 1 \quad (11)$$

$$xs_{j,h} = 0, \qquad ys_{j,h} = 0 \quad (12)$$

$$\left.\begin{array}{l} Ls_j^* = Vs_j^* + B_j^{rev} \\ Ls_j^* xs_{j,i}^* = Vs_j^* ys_{j,i}^* + B_j^{rev} x_{i,B_j}^{rev} \;\forall\, i \in C \\ Ls_j^* hs_{Lj}^* + Q_{Hj}^{rev} = Vs_j^* hs_{Vj}^* + B_j^{rev} h_{B_j} \end{array}\right\}$$
$$\forall\, j \in NCOL, j \le 2^{NC-2} - 1 \quad (13)$$

Figure 6. Control volume for the reversible exhausting point calculations.

$$\sum_{i=1}^{NC} xs_{j,i}^* = 1 \qquad \sum_{i=1}^{NC} ys_{j,i}^* = 1 \qquad (14)$$

$$xs_{j,1} = 0 \qquad ys_{j,1} = 0 \qquad (15)$$

Equations 10 and 11 are overall balances for the region involving the top part of the rectifying section of the column and the saddle pinch point zone. This region involves a condenser where the reversible energy Q_{Cj}^{rev} is exchanged. The equations in (12) impose the condition of an upper saddle pinch point occurrence. The heaviest component of the feed, "h", has to be completely removed when the saddle pinch point is reached. Equations 13 and 14 are the overall mass and energy balances for the stripping section region between the bottom part of the column and the zone where the lower saddle pinch point takes place. Note that the equations in (15) impose the condition that the lightest component of the feed entering column j, "l", is removed in the lower saddle pinch point region. The VLE equations are rigorously modeled using analogous equations to eqs 8 and 9. Note that the saddle pinch points have to be computed only for those columns located in zone A. The columns of the last level of the superstructure are fed by binary mixtures; therefore, saddle pinch points do not take place.

Next, the exhausting pinch point model (EPPM) to compute the reversible exhausting upper (lower) pinch point compositions $xp_{i,j}^D (xp_{i,j}^B)$, the liquid and vapor flow rates Lp_j and Vp_j (Lp_j^* and Vp_j^*), respectively, and energy demands $Q_{Cj}^{pinch}(Q_{Hj}^{pinch})$ is given next (see Figure 6):

EPPM:

$$\left.\begin{array}{l} F_j = D_j + B_j \\ F_j x_{j,i} = D_j xp_{i,j}^D + B_j xh_j \; \forall \; i \in C \\ F_j h_{F_j} + Q_{Hj}^{ind} + Q_{Cj}^{ind} = D_j h_{D_j} + B_j h_{B_j} \end{array}\right\}$$
$$\forall \; j \in NCOL, j \le 2^{NC-2} - 1 \quad (16)$$

$$\sum_{i=1}^{NC} xp_{i,j}^D = 1 \qquad (17)$$

$$\left.\begin{array}{l} F_j = D_j^* + B_j^* \\ F_j x_{j,i} = D_j^* xl_j + B_j^* xp_{i,j}^B \; \forall \; i \in C \\ F_j h_{F_j} + Q_{Hj}^{dir} + Q_{Cj}^{dir} = D_j^* h_{D_j} + B_j^* h_{B_j} \end{array}\right\}$$
$$\forall \; j \in NCOL, j \le 2^{NC-2} - 1 \quad (18)$$

$$\sum_{i=1}^{NC} xp_{i,j}^B = 1 \qquad (19)$$

$$\left.\begin{array}{l} Lp_j + D_j^{rev} = Vp_j \\ Lp_j xp_{i,j}^D + D_j^{rev} x_{i,D_j}^{rev} = Vp_j yp_{i,j}^D \; \forall \; i \in C \\ Lp_j hp_{L_j} + D_j^{rev} h_{D_j} = Vp_j hp_{Vj} + Q_{pj}^D \\ Q_{Cj}^{pinch} = Q_{Cj}^{rev} - Q_{pj}^D \end{array}\right\}$$
$$\forall \; j \in NCOL, j \le 2^{NC-2} - 1 \quad (20)$$

$$\left.\begin{array}{l} Lp_j^* = B_j^{rev} + Vp_j^* \\ Lp_j^* xp_{i,j}^B = B_j^{rev} x_{i,B_j}^{rev} + Vp_j^* yp_{i,j}^B \; \forall \; i \in C \\ Lp_j^* hp_{L_j}^* + Q_{pj}^D = B_j^{rev} h_{B_j} + Vp_j^* hp_{V_j}^* \\ Q_{H_j}^{pinch} = Q_{H_j}^{rev} - Q_{pj}^B \end{array}\right\}$$
$$\forall \; j \in NCOL, j \le 2^{NC-2} - 1 \quad (21)$$

First, the systems of equations given by (16) and (17) ((18) and (19)) are solved to calculate the composition of the reversible exhausting pinch point $xp_{i,j}^D (xp_{i,j}^B)$ that takes place in the rectifying (stripping) section. Note that a fictitious situation is considered to compute these compositions. The pinch is calculated for each column j as the distillate (bottom) composition emerging from a column where a high (low) boiler-rich bottom (distillate) is obtained. These assumptions are valid because of the straightness of the reversible path in the zone of interest (see Appendix A for demonstration). Note that $xl_j(xh_j)$ is the composition of the pure lightest (heaviest) product.

The equations in (20) are the overall balances formulated to a portion of a reversible rectifying zone involving the region where the upper reversible exhausting pinch takes place and the top part of the column (see Figure 6). The energy demand involved is Q_{pj}^D. For the stripping section of the column, eq 21 is applied. The VLE equations as well as the vapor and liquid enthalpies definitions are modeled with similar equations as eqs 8 and 9. Note that eqs 16−21 apply for all columns except those units located in the last level of the superstructure since reversible exhausting pinch points do not occur in zone B.

Sequence Preprocessing Phase. Consider the integration between the stripping section of column j and the rectifying section of column $j + 1$. Note that the same pure products emerge from section j and $j + 1$. The vapor V_j^* (liquid L_j^*) flow leaving (entering) the reversible stripping section of column j is used to compute the products flows pL_j and pV_j leaving an entering this section, respectively. The same holds for the rectifying section $j + 1$ (see Figure 7). The integration model (IM) is presented next:

IM:

$$\left.\begin{array}{l} L_j^* - V_j^* = pL_j - pV_j \\ L_j^* x_{j,i} - V_j^* y_{j,i} = pL_j x_{j,i}^l - pV_j y_{j,i}^v \; \forall \; i \in C \\ L_j^* h_{L_j} - V_j^* h_{V_j} + Q_{Hj}^{rev} = pL_j h_j^l - pV_j h_j^v \end{array}\right\}$$
$$\forall \; j \in NCOL, 2^{NC-2} \le j \le 2^{NC-1} - 1 \quad (22)$$
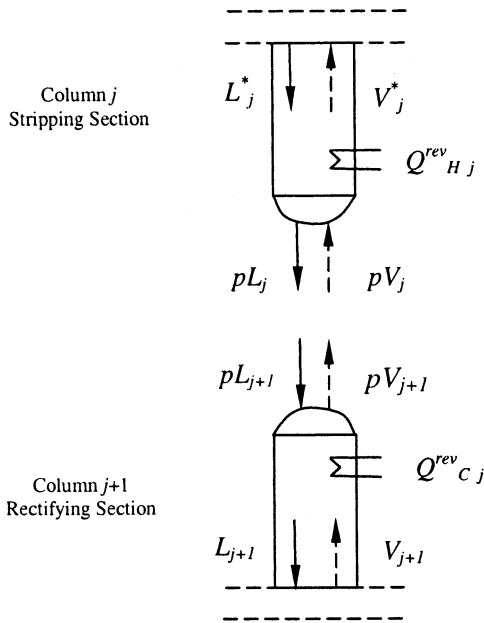
Figure 7. Control volumes for calculation of interconnections flows in zone B.

$$
\left.
\begin{aligned}
L_{j+1} - V_{j+1} &= pL_{j+1} - pV_{j+1} \\
L_{j+1}x_{j+1,i} - V_{j+1}y_{j+1,i} &= pL_{j+1}x^l_{j+1,i} - pV_{j+1}y^v_{j+1,i} \ \forall \ i \in C \\
L_{j+1}h_{L_{j+1}} - V_{j+1}h_{V_{j+1}} + Q^{rev}_{Cj+1} &= pL_{j+1}h^l_{j+1} - pV_{j+1}h^v_{j+1}
\end{aligned}
\right\}
$$

$$
\forall j \in \text{NCOL}, \ 2^{NC-2} \le j \le 2^{NC-1} - 1 \ (23)
$$

$$
Q_{\text{int }j} = Q^{rev}_{Hj} - Q^{rev}_{Cj+1}
$$

$$
\forall j \in \text{NCOL}, \ 2^{NC-2} \le j \le 2^{NC-1} - 1 \ (24)
$$

The equations in (22) are the overall balances formulated to the reversible stripping section of column j. The reversible rectifying section is modeled by eq 23. The energy exchanged after the integration of the stripping section of column j and the rectifying section of column $j + 1$ is $Q_{\text{int }j}$, which is defined by eq 24. Note that eqs 22−24 apply to all the columns in the last level of the superstructure, $2^{NC-2} \le j \le 2^{NC-1} - 1$ and j is even.

After the model (IM) is solved, the parameters defined in eq 25 can be computed. These parameters will be involved in the equations of the rigorous tray-by-tray synthesis model of section 5.2.

$$
\left.
\begin{aligned}
\text{pliq}_j &= pL_j - pL_{j+1} \\
\text{pvap}_j &= pL_{j+1} - pL_j \\
\text{signl}_j &= \frac{\text{pliq}_j}{\text{abs}(\text{pliq}_j)} \\
\text{signv}_j &= \frac{\text{pvap}_j}{\text{abs}(\text{pvap}_j)}
\end{aligned}
\right\}
$$

$$
\forall j \in \text{NCOL}, \ 2^{NC-2} \le j \le 2^{NC-1} - 1 \ (25)
$$

Note that the parameter $\text{pliq}_{j+1}(\text{pvap}_j)$ represents the net liquid (vapor) flow entering the top (bottom) of column $j + 1$ (j). The signs signl_j and signv_j will be involved in the equations which model the sections interconnections in zone B (see Figure 3) to provide the direction for the liking streams.

5.2. Rigorous Sequence Model. This section presents the formulation of the tray-by-tray mixed-integer nonlinear program which models the efficient super-structure proposed in section 3.

Given is a zeotropic feed with NC components with flow rate, composition, and enthalpy F_0, zf_{0i}, and hf_0, respectively. Consider a RDS-based superstructure with $2^{NC-1} - 1$ adiabatic columns and NC − 1 levels, as shown in Figure 8.

Consider the following sets definitions for the formulation of the model. Let NLEVEL be a level l of the superstructure: NLEVEL = $\{l|l = 1, 2, ..., L = NC − 1\}$. Let NF be the set of feeds nf, NF = $\{\text{nf}|\text{nf} = F, S, L\}$. Let the subsets NFp be the primary feeds: NFp = $\{\text{nf}|\text{nf} = F\}$. Let NP be the set of products np, NS be the set of trays n:NS = $\{n|n = 1, 2, ..., N\}$, REB be the candidate stages for placing a reboiler, and COND be the candidate stages for placing a condenser. Let top_j and bot_j be the top and bottom trays of column j, respectively. Let FEED$_{\text{nf},j}$ be the candidate trays n in column j of feed nf. Let the set SIDEP$_{\text{np}}$ be the stages from where a product np emerges. Then, PRODS = TOP ∪ BOT ∪$_{\text{np}}$ SIDEP$_{\text{np}}$.

Next, the complete formulation of the efficient sequence synthesis model (ESSM) is detailed.

The objective function of the problem is given by eq 26. The difference between each stream composition which connects the units with respect to the pinch points composition is minimized.

$$
\begin{aligned}
z_{\text{ESSM}} = &\sum_{i=1}^{NC}\left[\sum_{j=1}^{2^{NC-2}} (y_{\text{top}_j,i} - \text{yp}^D_{j,i})^2\right] + \\
&\left[\sum_{j=1}^{2^{NC-2}} (x_{\text{bot}_j,i} - \text{xp}^B_{j,i})^2\right] + \left[\sum_{\substack{j=2 \\ j\,\text{even}}}^{J} (\text{zf}_{Sj,i} - \text{xp}^D_{j,i})^2\right] + \\
&\left[\sum_{\substack{j=3 \\ j\,\text{odd}}}^{J} (\text{zf}_{Sj,i} - \text{yp}^B_{j,i})^2\right] + \left[\sum_{m=1}^{M} (\text{zP}_{m,i} - \text{xprod}_{m,i})^2\right] \ (26)
\end{aligned}
$$

The first term of eq 26 specifies the vapor composition $y_{\text{top}_j,i}$ to have a similar composition to the vapor emerging from the reversible exhausting pinch point region $\text{yp}^D_{j,i}$. The difference for the bottom products are expressed in the second term of this equation. Note that these terms are considered for those columns located in zone A of the superstructure. The recycle streams compositions are specified by the third and fourth term of eq 26. For even (odd) columns, the difference between the liquid (vapor) recycle composition $\text{zf}_{Sj,i}$ and the exhausting pinch point composition $\text{xp}^D_{j,i}$ ($\text{yp}^D_{j,i}$) is considered. Finally, in zone B of the superstructure, the difference between each final product composition $\text{zP}_{m,i}$ and the required purity $\text{xprod}_{m,i}$ are expressed. Note that the index m denotes each final product: FP = $\{m|m = 1, 2, ..., M = 3 \times 2^{NC-1}\}$.

Note that in eq 26 the reversible exhausting pinch points were used but the saddle pinch point composition can be used instead.

Mass and energy balances are formulated for every tray. The equations in (27) model the feed tray, the equations in (28) are applied to all trays from where side products emerge, the equations in (29) are applied to all intermediate trays, and eqs 30 and 31 model the top and bottom trays, respectively. Note that
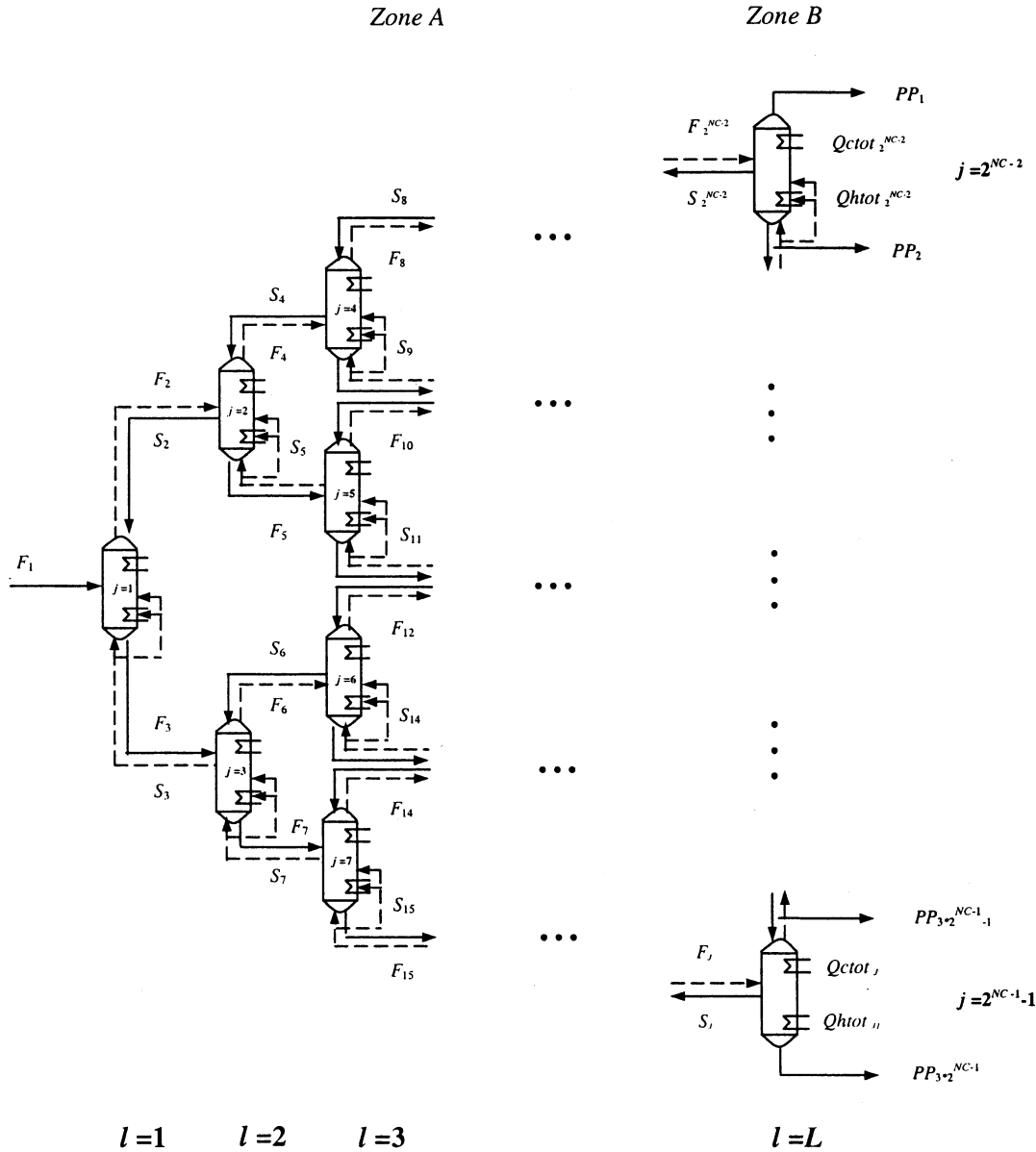
Zone A   *Zone B*

Figure 8. General RDSM-based superstructure.

$$\text{TOP} = \cup_{j=1}^{J} \text{top}_j, \quad \text{BOT} = \cup_{j=1}^{J} \text{bot}_j \text{ and NIT} = \text{NS} - \{\text{TOP} \cup \text{BOT} \cup_j \text{FEED}_{\text{nf},j} \cup_j \text{SIDEP}_{\text{np},j}\}.$$

$$\left. \begin{array}{r} \displaystyle\sum_{\text{nf} \in \text{FEED}_{\text{nf},j}} F_{\text{nf},n} \text{zf}_{\text{nf},i} + L_{n-1} x_{n-1,i} + V_{n+1} y_{n+1,i} - \\ L_n x_{n,i} - V_n y_{n,i} = 0 \ \forall \ i \in C \\ \displaystyle\sum_{\text{nf} \in \text{FEED}_{\text{nf},j}} F_{\text{nf},n} \text{hf}_{\text{nf}} + L_{n-1} \text{hl}_{n-1} + V_{n+1} \text{hv}_{n+1} - \\ L_n \text{hl}_n - V_n \text{hv}_n = 0 \end{array} \right\}$$
$$\forall \ n \in \text{FEED}_{\text{nf},j} \quad (27)$$

$$\left. \begin{array}{l} L_{n-1} x_{n-1,i} + V_{n+1} y_{n+1,i} - (L_n + \text{PL}_n) x_{n,i} - (V_n + \text{PV}_n) y_{n,i} \ \forall \ i \in C \\ L_{n-1} \text{hl}_{n-1} + V_{n+1} \text{hv}_{n+1} - (L_n + \text{PL}_n) \text{hl}_n - (V_n + \text{PV}_n) \text{hv}_n \end{array} \right\}$$
$$\forall \ n \in \text{SIDEP}_{\text{np},j} \quad (28)$$

$$\left. \begin{array}{l} L_{n-1} x_{n-1,i} + V_{n+1} y_{n+1,i} = L_n x_{n,i} + V_n y_{n,i} \ \forall \ i \in C \\ L_{n-1} \text{hl}_{n-1} + V_{n+1} \text{hv}_{n+1} = L_n \text{hl}_n + V_n \text{hv}_n \end{array} \right\}$$
$$\forall \ n \in \text{NIT} \quad (29)$$

$$\left. \begin{array}{l} L_n x_{n,i} + \text{PL}_n x_{n,i} + \text{PV}_n y_{n,i} - V_{n+1} y_{n+1,i} = 0 \ \forall \ i \in C \\ L_n \text{hl}_n + \text{PL}_n \text{hl}_n + \text{PV}_n \text{hv}_n - Q_n - V_{n+1} \text{hv}_{n+1} = 0 \end{array} \right\}$$
$$\forall \ n \in \text{TOP} \quad (30)$$

$$\left. \begin{array}{l} V_n y_{n,i} + \text{PL}_n x_{n,i} - L_{n-1} x_{n-1,i} = 0 \ \forall \ i \in C \\ \text{PL}_n \text{hl}_n + V_n \text{hv}_n + \text{PV}_n \text{hv}_n - Q_n - L_{n-1} \text{hl}_{n-1} = 0 \end{array} \right\}$$
$$\forall \ n \in \text{BOT} \quad (31)$$

The VLE equations, the summation of mole fractions, and the definitions of the enthalpies for the internal vapor and liquid stream are given by eqs 32, 33, and 34, respectively. Ideal VLE is adopted.

$$\left. \begin{array}{l} f_{n,i}^L = f(T_n, P_n, x_{n,i}) \\ f_{n,i}^V = f(T_n, P_n, y_{n,i}) \\ f_{n,i}^L = f_{n,i}^V \end{array} \right\} \forall \ n \in \text{NS}, i \in C \quad (32)$$

$$\sum_{i=1}^{NC} x_{n,i} = 1 \atop \sum_{i=1}^{NC} y_{n,i} = 1 \Bigg\} \forall\, n \in NS \qquad (33)$$

$$\begin{aligned} hv_n &= f(T_n) \\ hl_n &= f(T_n) \end{aligned} \Bigg\} \forall\, n \in NS \qquad (34)$$

The energy demands involved in the condenser $Qctot_j$ and reboiler $Qhtot_j$ of every column j are defined in eq 35:

$$\begin{aligned} Qhtot_j &= \sum_{n \in reb_j} Q_n \\ Qctot_j &= \sum_{n \in cond_j} Q_n \end{aligned} \Bigg\} \forall\, j \in NCOL \qquad (35)$$

Total mass and energy balances are formulated for the superstructure in eqs 36. In constraints (37), mass and energy balances are formulated for each column of the superstructure:

$$\sum_{n \in feed_{F_1,1}} F_{F_1,n} = \sum_{m=1}^{M} PP_m$$

$$\sum_{n \in feed_{F_1,1}} F_{F_1,n} zf_{nf,i} = \sum_{m=1}^{M} PP_m zP_{m,i} \;\forall\, i \in C$$

$$\sum_{n \in feed_{F_1,1}} F_{F_1,n} hf_{F_1,n} + \qquad (36)$$

$$\sum_{j=1}^{J}(Qhtot_j - Qctot_j) = \sum_{m=1}^{M} PP_m hP_m$$

$$\begin{aligned} \sum_{n \in N_j} \sum_{nf \in FEED_{nf,j}} F_{n,i} zf_{nf,i} &= \sum_{n \in N_j}(PL_n + PV_n) \;\forall\, i \in C \\ \sum_{n \in N_j} \sum_{nf \in feed_{nf,j}} F_{n,i} hf_{nf} + Qhtot_j - Qctot_j &= \sum_{n \in N_j}(PL_n hl_n + PV_n hv_n) \end{aligned} \Bigg\}$$

$$\forall\, j \in NCOL \quad (37)$$

Column interconnection balances are considered next. The problem feed flow, composition, and enthalpy are defined in eq 38:

$$\sum_{n \in FEED'_{F1',j}} F'_{F1',n} = F_0$$

$$zf_{F1',i} = zf_{0i} \quad \forall\, i \in C \qquad (38)$$

$$\sum_{n \in FEED'_{F1',j}} hf_{F1',n} = hf_0$$

Primary feeds are defined by eq 39. The liquid (vapor) product emerging from the top (bottom) of a column becomes the feed of a subsequent column of the superstructure.

$$\begin{aligned} PV_{top_j} &= \sum_{n \in FEED_{F2,j,j}} F'_{F_{2j',n}} \\ y_{top_j,i} &= zf_{F_{2j'},i} \;\forall\, i \in C \\ hv_{top_j} &= hf_{F_{2j'}} \\ PL_{bot_j} &= \sum_{nf \in FEED'_{F2,j+1',j}} F'_{F_{2j+1'},n} \\ x_{bot_j,i} &= zf_{F_{2j+1'},i} \;\forall\, i \in C \\ hl_{bot_j} &= hf_{F_{2j+1'}} \end{aligned} \Bigg\}$$

$$\forall\, j \in NCOL,\, 1 \le j \le J - 1 \quad (39)$$

Secondary feeds are defined in eqs 40 and 41. The liquid (vapor) side product becomes the secondary feed of a preceding column in the superstructure.

$$\begin{aligned} \sum_{n \in SIDEP'_{Sj,j}} PL_n &= \sum_{n \in FEED'_{Sj,j}} F'_{S_j',n} \\ \sum_{n \in SIDEP'_{Sj,j}} PL_n x_{n,i} &= \sum_{n \in FEED'_{Sj}} F'_{S_j',n} zf_{S_j',i} \;\forall\, i \in C \\ \sum_{n \in SIDEP'_{Sj,j}} PL_n hl_n &= \sum_{n \in FEED'_{Sj,j}} F'_{S_j',n} hf_{S_j'} \end{aligned} \Bigg\}$$

$$\forall\, j \in NCOL,\, 2 \le j \le J,\, j\,\text{even} \quad (40)$$

$$\begin{aligned} \sum_{n \in SIDEP_{Sj,j}} PV_n &= \sum_{n \in FEED_{Sj,j}} F'_{S_j',n} \\ \sum_{n \in SIDEP_{Sj,j}} PV_n y_{n,i} &= \sum_{n \in FEED_{Sj,j}} F'_{S_j',n} zf_{S_j',i} \;\forall\, i \in C \\ \sum_{n \in SIDEP_{Sj,j}} PV_n hv_n &= \sum_{n \in FEED_{Sj,j}} F'_{S_j',n} hf_{S_j'} \end{aligned} \Bigg\}$$

$$\forall\, j \in NCOL,\, 3 \le j \le J,\, j\,\text{odd} \quad (41)$$

The balances for those sections which are integrated are modeled from eqs 42−49 (see Figure 3). Equation 42 defines the secondary feeds $F_{L_j,n}$ and $F_{L_j+1,n}$. Note that the parameters $signl_j$ and $signv_j$ were defined in eq 25.

$$\begin{aligned} PL_{bot_j} - \sum_{n \in FEED'_{Lj}} F'_{L_j',n} &= signl_j ppl_j \\ PL_{bot_j} x_{bot_j,i} - \sum_{n \in FEED'_{Lj}} F'_{L_j',n} zf_{L_j',i} &= signl_j ppl_j zpl_{j,i} \;\forall\, i \in C \\ PL_{bot_j} hl_{bot_j} - \sum_{n \in FEED'_{Lj}} F'_{L_j',n} hf_{L_j'} &= signl_j ppl_j hpl_j \\ PV_{top_{j+1}} - \sum_{n \in FEED'_{Lj+1'}} F'_{L_{j+1'},n} &= signv_j ppv_j \\ PV_{top_{j+1}} x_{top_{j+1},i} - \sum_{n \in FEED'_{Lj+1'}} F'_{L_{j+1'},n} zf_{L_{j+1'},i} &= signv_j ppv_j zpv_{j,i} \;\forall\, i \in C \\ PV_{top_{j+1}} hv_{top_{j+1}} - \sum_{n \in FEED'_{Lj+1'}} F'_{L_{j+1'},n} hf_{L_{j+1'}} &= signv_j ppv_j hpv_j \end{aligned} \Bigg\}$$

$$\forall\, j \in NCOL,\, j \in \{2^{NC-1} - 1 - NC + t\},$$
$$0 \le t \le J - 1,\, t\,\text{even} \quad (42)$$

The energy demanded in the integration of column j and column $j + 1$, $Q_{\text{phase }j}$, is defined in eqs 43 and 44 according to the values of the parameters $pvap_j$ and $pliq_j$ previously computed in the preprocessing phase formu-

lations (see eq 25). Note that the condensation enthalpy $\Delta Hcond_j$ is a parameter in the model.

$$Q_{\text{phase } j} = ppv_j\Delta Hcond_j \,\forall\, j \in \text{NCOL},\, j \in$$
$$\{2^{\text{NC}-1} - 1 - \text{NC} + t\},$$
$$0 \le t \le J - 1,\, t\text{ even},\, pvap_j > 0 \quad (43)$$

$$Q_{\text{phase } j} = -ppl_j\Delta Hcond_j \,\forall\, j \in \text{NCOL},\, j \in$$
$$\{2^{\text{NC}-1} - 1 - \text{NC} + t\},$$
$$0 \le t \le J - 1,\, t\text{ even},\, pliq_j > 0 \quad (44)$$

The equations in (45) define the products emerging from totally integrated sections (see Figure 3).

$$\left.\begin{array}{l}
signl_j ppl_j + signv_j ppv_j = PP_m \\
signl_j ppl_j zpl_{j,i} + signv_j ppv_j zpv_{j,i} = PP_m zP_{m,i} \,\forall\, i \in C \\
signl_j ppl_j hpl_j + signv_j ppv_j(hpv_j + \Delta Hcond_j) = PP_m hP_m
\end{array}\right\}$$
$$\forall\, j \in \text{NCOL},\, m \in \text{FP},\, j \in \{2^{\text{NC}-1} - 1 - \text{NC} + t\},$$
$$m = 3t - 1,\, 0 \le t \le K - 1,\, t\text{ even} \quad (45)$$

Constraints (46) define the final product reach in the lightest component:

$$\left.\begin{array}{l}
PP_m = PL_{\text{top}_1} \\
PP_m zP_{m,i} = PL_{\text{top}_1}x_{\text{top}_1,i} \,\forall\, i \in C \\
PP_m hP_m = PL_{\text{top}_1}hl_{\text{top}_1}
\end{array}\right\}\forall\, m \in \text{FP},\, m = 1$$
$$(45)$$

Constraints (47) define the final product reach in the heaviest component:

$$\left.\begin{array}{l}
PP_m = PL_{\text{bot}_J} \\
PP_m zP_{m,i} = PL_{\text{bot}_J}x_{\text{bot}_J,i} \,\forall\, i \in C \\
PP_m hP_{m,i} = PL_{\text{bot}_J}hl_{\text{bot}_J}
\end{array}\right\}\forall\, m \in \text{FP},\, m = J$$
$$(47)$$

In the equations in (48), the top liquid products emerging from nonintegrated rectifying sections are defined as follows:

$$\left.\begin{array}{l}
PP_m = PL_{\text{top}_j} \\
PP_m zP_{m,i} = PL_{\text{top}_j}x_{\text{top}_j,i} \,\forall\, i \in C \\
PP_m hP_m = PL_{\text{top}_j}hl_{\text{top}_j}
\end{array}\right\}$$
$$j \in \text{NCOL},\, m \in \text{FP},\, j \in \{J - \text{NC} + 2 + t\},$$
$$J - \text{NC} + 2 \le j \le J - 1,\, m \ge 4,\, t \ge 0,\, t\text{ even} \quad (48)$$

In eq 49, the final products are defined for nonintegrated stripping sections:

$$\left.\begin{array}{l}
PP_m = PL_{\text{bot}_j} \\
PP_m zP_{m,i} = PL_{\text{bot}_j}x_{\text{bot}_j,i} \,\forall\, i \in C \\
PP_m hP_m = PL_{\text{bot}_j}hl_{\text{bot}_j}
\end{array}\right\}$$
$$\forall\, j \in \text{NCOL},\, m \in \text{FP},\, j \in \{J - \text{NC} + 1 + t\},$$
$$J - \text{NC} + 1 \le j \le J - 1,\, m \ge 3,\, t \ge 0,\, t\text{ even} \quad (49)$$

Logical constraints given by eqs 50, 51, and 52, are introduced to model variable feed, product withdrawal, and heat exchange equipments locations. Binary variable $bf_{\text{nf},n}$, $bp_{\text{np},n}$, and $bheat_n$ are defined to denote whether a stage is or not a stage where a feed enters, a product emerges, or heat exchange takes place, respectively. Conditions imposing only one feed stage, one side product stage, and one stage for placing the reboiler are allowed, respectively.

$$\left.\begin{array}{l}
F_{\text{nf},n} = bf_{\text{nf},n}Fmax_{\text{nf}} \,\forall\, n \in \text{FEED}_{\text{nf},j} \\
\displaystyle\sum_{n\in\text{FEED}_{\text{nf},j}} bf_{\text{nf},n} = 1
\end{array}\right\}\forall\, \text{nf} \in \text{NFp} \quad (50)$$

$$\left.\begin{array}{l}
q_{\text{np}}PV_n + (1 - q_{\text{np}})PL_n \le bp_{\text{np},n}Pmax_{\text{np}} \,\forall\, n \in \text{SIDEP}_{\text{np},j} \\
\displaystyle\sum_{n\in\text{SIDEP}_{\text{np},j}} bp_{\text{np},n} = 1
\end{array}\right\}$$
$$\forall\, \text{np} \in \text{NP} \quad (51)$$

$$\left.\begin{array}{l}
Q_n \le bheat_n Qmax \quad \forall\, n \in \text{REB} \\
\displaystyle\sum_{n\in\text{reb}_j} bheat_n = 1
\end{array}\right.$$
$$(52)$$

6. Solution of Models

6.1. Preprocessing Phase. In this section, a solution procedure for the preprocessing formulations (see section 5.1) is proposed. The reversible-based superstructure can be initialized in various ways. In this paper, a successive procedure is adopted and an algorithmic procedure is derived. The advantage of choosing a successive procedure relies on the fact that the values computed at one step can be used as initial values in the next step of calculation.

The procedure to solve the preprocessing phase is presented next and summarized in Figure 9. It should be noted that as it was mentioned in section 5.1, the problem feed flow, composition, and enthalpy are known.

The algorithm to solve the preprocessing models is presented next:

Initialization Step:
Let $l = 1$ and $j = 1$. Calculate the reversible products, saddle, and reversible exhausting pinch points, solving the models TRM, SPPM, and EPPM, respectively.

Main Step:
Iteration k. Let l be the actual level of the superstructure. Set $j = 2^{l-1}$, which is the first column in level l. Note that j is even.
1. Compute the mole flow and composition of the fictitious feed entering column j using eq 53.

$$\left.\begin{array}{l}
Fcol_j = Vp_{j/2} - Lp_{j/2} \\
zcol_{j,i} = \dfrac{Vp_{j/2}yp^D_{i,j/2} - Lp_{j/2}xp^D_{i,j/2}}{Vp_{j/2} - Lp_{j/2}} \,\forall\, i \in \text{NC} \\
q_j = \dfrac{Vp_{j/2}}{Vp_{j/2} - Lp_{j/2}}
\end{array}\right\}$$
$$\forall\, j \in \text{NCOL},\, j\text{ even} \quad (53)$$

Solve a flash model for the feed defined in eq 53 to compute $x^F_{j,i}$, $y^F_{j,i}$, h_{L_j}, and h_{V_j}.

Solve TRM for calculating the reversible products, SPPM to compute the saddle (for scenarios 1 and 2) or EPPM reversible exhausting points (for scenario 3).

Compute the next value for the set j as $j = j + 2$.

—If $j = 2^l - 1$, which is the last even column in level l, go to step 2. Otherwise, repeat step 1.

2. Let $j = 2^{l-1} + 1$, which is the first odd column in level l. Compute the fictitious feed entering to column j as

$$\left. \begin{aligned} \text{Fcol}_j^* &= \text{Lp}_{(j-1)/2}^* - \text{Vp}_{(j-1)/2}^* \\ \text{zcol}_{j,i}^* &= \frac{\text{Lp}_{(j-1)/2}^* x p_{i,(j-1)/2}^B - \text{Vp}_{(j-1)/2}^* y p_{i,(j-1)/2}^B}{\text{Lp}_{(j-1)/2}^* - \text{Vp}_{(j-1)/2}^*} \\ q_j^* &= 1 - \frac{\text{Lp}_{(j-1)/2}^*}{\text{Lp}_{(j-1)/2}^* - \text{Vp}_{(j-1)/2}^*} \end{aligned} \right\} \quad (54)$$

Solve a flash model for the feed defined in eq 54 to compute $x_{j,i}^F$, $y_{j,i}^F$, h_{L_j}, and h_{V_j}.

Solve TRM for calculating the reversible products, SPPM to compute the saddle (for scenario 1 and 2) or EPPM reversible exhausting points (for scenario 3).

Compute the next value of j as $j = j + 2$.

—If $j > 2^l - 1$, go to the following level. Set $l = l + 1$.

—If $l = \text{NC} - 1$, which is the last level of the sequence, go to step 3.

—Otherwise, set $j = 2^{l-1}$ and go to step 1.

—Otherwise, repeat step 2.

3. Set $j = 2^{\text{NC}-2}$, which is the first column in the last level of the sequence. Compute $Q_{\text{int } j} = Q_{Hj}^{\text{rev}} - Q_{Cj+1}^{\text{rev}}$.

—If $Q_{\text{int}} < 0$, then $Q_{Cj+1}^{\text{rev}} = Q_{\text{int } j}$ and $Q_{Hj}^{\text{rev}} = 0$.

—Otherwise, $Q_{Cj+1}^{\text{rev}} = 0$ and $Q_{Hj}^{\text{rev}} = Q_{\text{int } j}$.

Solve IM to compute the molar flow emerging from and entering column j integrated with column $j + 1$. Update the set $j = j + 2$.

—If $j > 2^{\text{NC}-1} - 1$, stop.

—Otherwise, repeat step 3.

6.2. Sequence Model Solution. After the preprocessing phase is solved, the rigorous tray-by-tray model presented in section 5.2 is solved as a MINLP problem.

The preprocessing phase solution is used to initialize and bound the variables of the sequence model. The solutions of the saddle pinch point model, the reversible exhausting point model, and the integration model are used to provide initial values and bounds for the heat loads, the products and secondary feeds composition, and flow rates. This initialization scheme leads the solution of the rigorous model to the RDS-based.

As was previously mentioned, three different RDS-based scenarios are studied involving different extents of the columns integration. In zone A, the interconnecting flows are desired to have the composition and flow rate similar to the saddle pinch point vapor in the case of dealing with scenario 1 or 2. In the case of scenario 3, the reversible exhausting pinch point compositions are specified. Note that, in all the scenarios, the flows interconnecting one unit with a previous one are in equilibrium.

For scenarios 1 and 2, upper bounds for the heat loads were set on the reversible values Q_{Cj}^{rev} and Q_{Hj}^{rev} (see eqs 10 and 13). As lower bounds, small values different from zero were used. Despite no heat exchange being involved in some columns in these scenarios, a zero value is not used because the RDS-based rigorous approximation

provides an initial solution guess for the economic optimization design. If the total cost of the sequence is minimized, some other configurations with different heat distribution may result. To not lose information on the original superstructure, small values for the heat loads are used.

For scenario 3, it is desired that the streams feeding and leaving the columns located in zone A have a similar composition and flow rates to those of the reversible exhausting points. As in the previous cases, the interconnecting flows composition and rates are initialized and bounded using the reversible exhausting point model solutions. The condenser and reboiler heat loads of column 1 are bounded around the values Q_{Cj}^{pinch} and Q_{Hj}^{pinch}, respectively (see eqs 20 and 21).

In the units located in zone B, liquid products emerge from the top or bottom if the column sections are not heat-integrated. In these cases, the reversible heat loads computed in the preprocessing phase are used for bounding. For integrated sections, the heat exchanged is $Q_{\text{int } j}$ (see eq 24). If $Q_{\text{int } j} < 0$, then the condenser heat load of column $j + 1$, $Q\text{ctot}_j$, is bounded around $Q_{\text{int } j}$ and the reboiler heat load, $Q\text{htot}_j$, is lower bounded at a small value different from zero. Otherwise, if $Q_{\text{int } j} > 0$, the energy exchanged in the reboiler, $Q\text{htot}_j$, is bounded around $Q_{\text{int } j}$.

7. Numerical Examples

The formulations presented were solved according to the solution scheme proposed in this work. Zeotropic mixtures involving different ease of separation indices (ESI)[11] were used to compute the entropy produced in each of the scenarios presented in Figure 4 (see Appendix B for a definition of ESI).

The scenarios presented in Figure 4 were tested with the methodology proposed in this paper. The following mixtures were considered: n-pentane/n-hexane/n-heptane (nnn, ESI ≈ 1); n-butane/isopentane/n-hexane (nin, ESI < 1); n-butane/isopentane/n-pentane (ESI > 1). See Appendix C for a detailed derivation of the expression to compute the entropy generation. A constant pressure of 1.01 bar and a feed flow of 10 mol/s are considered. In all cases, pure saturated liquid products are specified, with a recovery and purity of 98% in each component. In the examples, ideal equilibrium is used. The thermodynamic properties are taken form Reid et al.[12] In all cases, the VLE equations involve the transformation of variables suggested by Bauer and Stilchmair[13] to improve the convergence of the NLP problems. This transformation yields to more linear equations when modeling the VLE equations. Many different compositions were used to test the efficiency of the proposed scenarios. All the examples were implemented and solved in GAMS[14] in a PIII, 640 K, 500 MHz. The code DICOPT was employed for solving the MINLP problem and CONOPT for the NLP subproblems.

The following conclusions can be stated:

(1) Scenario 1 is the least efficient sequence.

(2) For zeotropic mixtures with ESI < 1 and ESI > 1, in all ranges of compositions, scenario 3 leads to the most efficient sequence.

(3) For zeotropic mixtures with ESI close to 1, in almost all cases, scenario 3 turns out to be the most efficient scheme. However, according to our experience, scenario 2 is the sequence with the lowest entropy
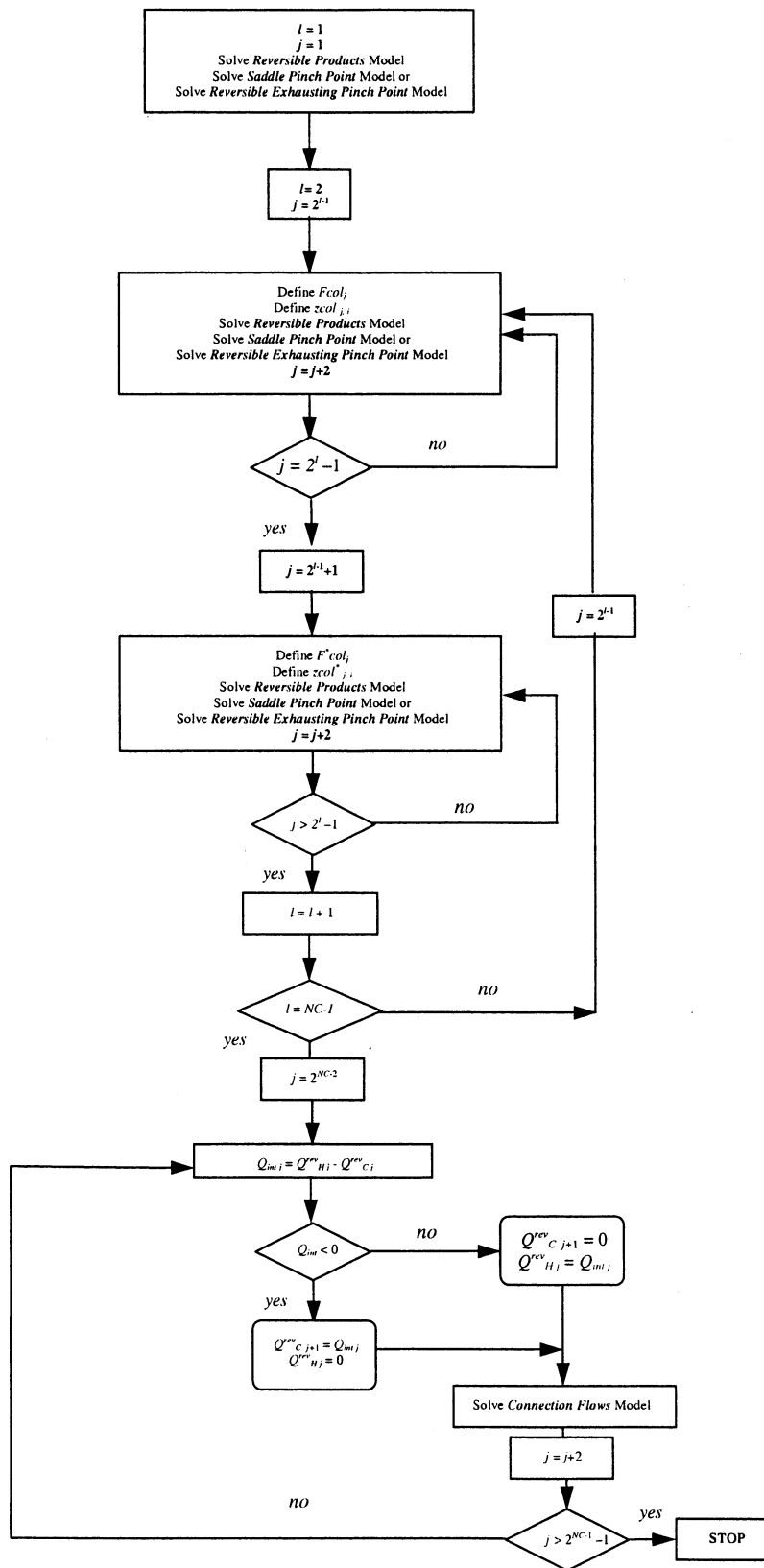
Figure 9. Algorithmic solution procedure to solve the preprocessing phase.

production in those cases when a mixture where the heaviest component is the most abundant species in the mixture.

(4) Scenario 2 is the configuration that involves the lowest total energy demand. However, scenario 3 is the most efficient representation. According to our experi-

ence, the total heat loads involved in scenario 3 are only 0.5–10% higher than the energy involved in scenario 2.

According to these conclusions, we consider that scenario 3 is the scheme which approaches more closely reversible conditions. Note that the total energy demand

**Table 1. Optimal Solutions—Feeds and Products Streams**

	flow rate		composition		
stream	theoretical	MINLP model	theoretical	MINLP model	feed tray
		Case 1: *n*-Pentane, *n*-Hexane, *n*-Heptane 0.1/0.1/0.8			
F_2	1.46	1.47	0.747/0.252/0	$0.748/0.252/2 \times 10^{-5}$	40
F_3	10.81	11.03	0/0.11/0.889	$4 \times 10^{-4}/0.113/0.886$	26
S_2	0.18	0.20	0.5/0.5/0	$0.5/0.499/4 \times 10^{-5}$	1
S_3	2.09	2.3	0/0.228/0.771	$1 \times 10^{-4}/0.226/0.773$	30
L_3	0.55	0.48	0/1/0	$1 \times 10^{-3}/0.998/2 \times 10^{-4}$	80
L_2	0.87	0.79	0/1/0	$1 \times 10^{-3}/0.998/9 \times 10^{-5}$	1
ppl	0.05	0.04	0/1/0	$1 \times 10^{-3}/0.998/9 \times 10^{-5}$	
ppv	1.05	0.98	0/1/0	$1 \times 10^{-3}/0.998/2 \times 10^{-4}$	
		Case 2: *n*-Butane, Isopentane, *n*-Pentane 0.33/0.33/0.34			
F_2	5.97	6.09	0.739/0.2603/0	$0.739/0.256/3 \times 10^{-3}$	42
F_3	9.39	9.49	0/0.4925/0.507	$4 \times 10^{-4}/0.497/0.502$	41
S_2	2.23	2.45	0.5/0.5/0	$0.495/0.5/6 \times 10^{-3}$	1
S_3	3.13	3.13	0/0.563/0.436	$9 \times 10^{-5}/0.563/0.436$	40
L_3	0.89	0.98	0/1/0	$5 \times 10^{-4}/0.995/4 \times 10^{-3}$	80
L_2	0.55	0.59	0/1/0	$4 \times 10^{-4}/0.992/7 \times 10^{-3}$	1
ppl	0.78	0.73	0/1/0	$4 \times 10^{-4}/0.992/7 \times 10^{-3}$	
ppv	2.52	2.57	0/1/0	$5 \times 10^{-4}/0.995/4 \times 10^{-3}$	
		Case 3: *n*-Pentane, *n*-Hexane, *n*-Heptane 0.3/0.5/0.2			
F_2	5.34	5.36	0.6355/0.364/0	$0.634/0.3652/6 \times 10^{-4}$	40
F_3	8.16	8.08	0/0.7143/0.2857	$4 \times 10^{-3}/0.71/0.2856$	26
S_2	1.05	1.15	0.375/0.625/0	$0.3733/0.6257/9 \times 10^{-4}$	1
S_3	2.45	2.29	0/0.864/0.1356	$1 \times 10^{-3}/0.863/0.1356$	30
L_3	1.88	1.77	0/1/0	$2 \times 10^{-3}/0.997/7 \times 10^{-4}$	80
L_2	2.49	2.4	0/1/0	$2 \times 10^{-3}/0.997/1 \times 10^{-3}$	1
ppl	0.67	0.6	0/1/0	$2 \times 10^{-3}/0.997/1 \times 10^{-3}$	
ppv	4.33	4.42	0/1/0	$2 \times 10^{-3}/0.997/7 \times 10^{-4}$	

involved in this scheme is close to the energy involved in Scheme 2, which is the lowest.[15,16]

Three examples solved with scenario 3 are presented in detail. Example 1 involves the separation of *n*-pentane, *n*-hexane, and *n*-heptane with composition 0.1/0.1/0.8 and uses ideal equilibrium. An upper number of trays of 30, 80, and 50 trays were selected for columns 1, 2, and 3, respectively. Example 2 deals with the separation of *n*-butane, isopentane, and *n*-pentane with composition 0.33/0.33/0.34. The upper number of trays used in units 1, 2, and 3 are 40, 80, and 80, respectively. Finally, example 3 is concerned with the separation of a mixture of *n*-pentane, *n*-hexane, and *n*-heptane with composition 0.3/0.5/0.2. In this example, the number of trays is 30, 80, and 50 for columns 1, 2, and 3, respectively. In all the examples, the pinch point occurrence criterion[9] was used to select upper bounds for the number of trays.

The superstructure of the problems is shown in Figure 10. Variable location for the primary and secondary feeds as well for the side products withdrawn is considered. The condensers are fixed while the reboilers locations are variable.

In Table 1, the solutions for the feeds and products streams are presented. Note that the flow rates and compositions obtained with the model are very close to the theoretical values computed in the preprocessing phase. In Table 2, the energy demand involved in each example is shown. The configurations for the examples are shown in Figure 11. Note that the configurations for examples 1 and 3 are similar. The integration of the reboiler of column 2 with column 3 condenser gives rise to a resultant energy exchanged in the condenser of unit 3. Also note that part of the vapor flow connecting both units provides flow to the main product PP$_2$ after its condensation. In example 2 part of the vapor leaving column 3 is condensed to provide the liquid reflux for the column and the other part constitutes pure isopentane product. Note that in example 1 and example 3
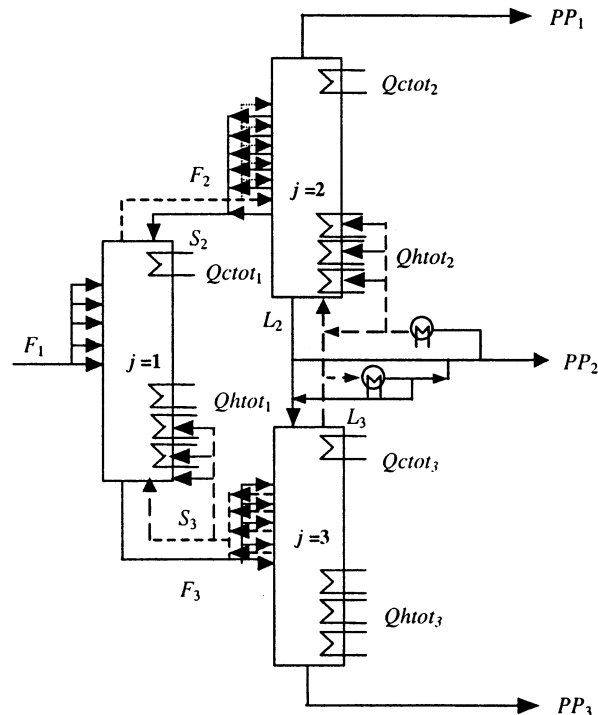
Figure 10. Scenario 3 superstructure for a ternary mixture.

the solutions involve minimum energy demand while in example 2 the heat loads are close to the minimum reflux conditions (see Table 2). In fact, the mixture of example 2 presents smaller differences between the relative volatility of its components. Then, a larger number of stages in columns 2 and 3 could be used if closer energy demands to the theoretical values are desired.

It is worth noting that due to the nature of the objective function, there is a tendency for the reboilers to be located in the bottom tray of each column in the
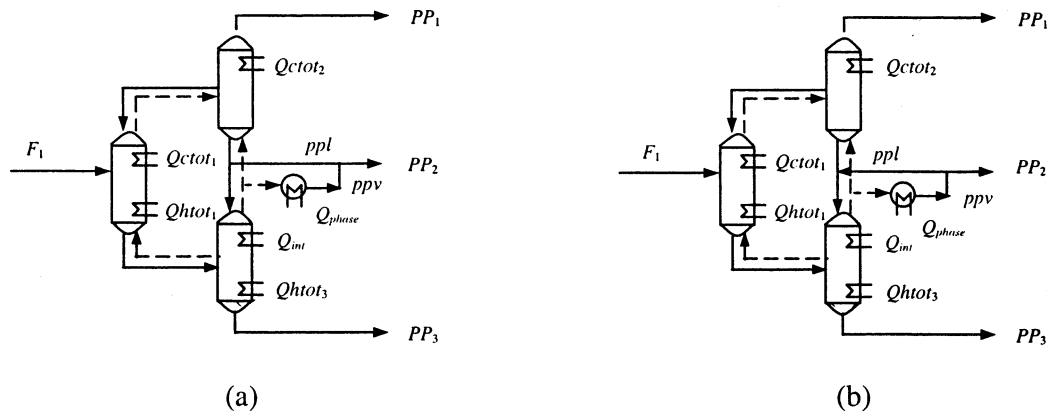
Figure 11. Efficient configurations. (a) Examples 1 and 3. (b) Example 2.

Table 2. Optimal Solutions—Energy Demand

heat duty	case 1 energy demand theoretical	case 1 energy demand MINLP model	case 2 energy demand theoretical	case 2 energy demand MINLP model	case 3 energy demand theoretical	case 3 energy demand MINLP model
$Qctot_1$	−60.26	−66.28	−38.78	−40.72	−16.63	−18.29
$Qhtot_1$	52.07	51.13	109.6	115.06	107.21	114.57
$Qctot_2$	−56.30	−56.12	−164.5	−167.7	−204.3	−203
$Qhtot_2$		1.8		1		1
$Qctot_3$	−139.71	−118.75	−430.7	−460	−50.27	−57.81
$Qhtot_3$	249.61	239.74	606	624	293.4	313.78

thermodynamic optimal solution. This is because there are no costs functions involved in the objective function. Then, the columns keep the upper bound in the number of trays initially selected.

In Table 3, the main products composition and flow rates are shown. The model size and the solution times for the three examples including the preprocessing phase are presented in Table 4.

8. Conclusions

This paper has presented an automatic procedure for the synthesis of efficient zeotropic distillation processes. A general superstructure based on the RDSM was proposed and rigorously modeled as an MINLP problem.

The formulation involves integration between columns as well as variable locations for feeds, reboilers, and side products. The solution procedure includes a preprocessing phase, where well-behaved NLP problems are successively solved to compute relevant values to initialize and bound the variables of the MINLP problem. An algorithmic procedure was proposed to automatically solve these preliminary calculations.

Numerical examples for ternary zeotropic mixtures were presented. Small solution times were involved; however, highly nonlinear and nonconvex formulations were solved. We have found that the fact of including the preprocessing phase enhances the convergence and robustness of the MINLP formulations.

Three scenarios with different energy distribution were analyzed and the efficiency related to each one was computed. According to our experience, the scheme which closer approximates reversible conditions involves energy exchange in all sections, except for those which are integrated.
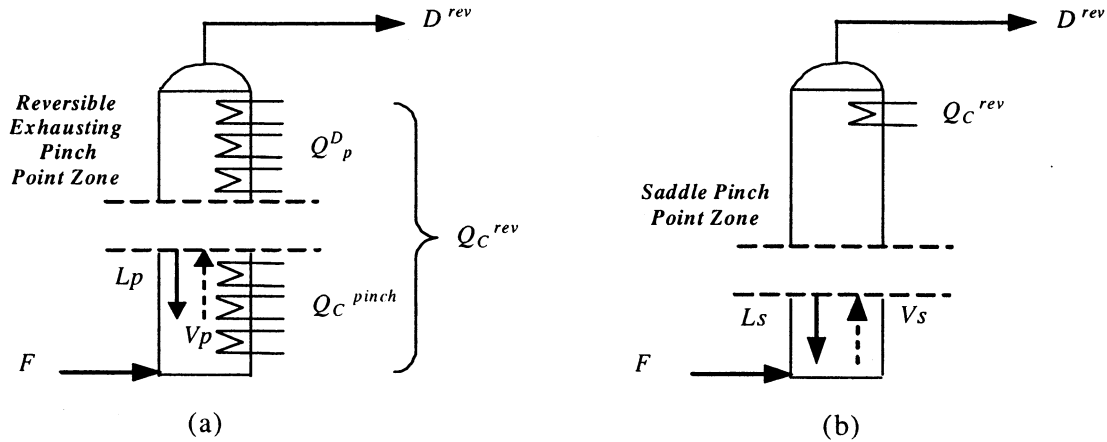
Since efficient designs keep all the elements of the initial superstructure, they can be used as initial solutions for the synthesis problem of complex columns configurations, where economic-based objective functions are minimized.

Appendices

Appendix A: Reversible Exhausting Pinch Points. Consider the rectifying section of an adiabatic and a reversible unit shown in Figure 12. In the reversible rectifying section (see Figure 12a), the total energy Q_C^{rev} is continuously distributed. In contrast, in the adiabatic rectifying section, where the reversible separation task is performed, the same amount of

Table 3. Optimal Solutions—Main Products

product	case 1 flow rate	case 1 composition	case 2 flow rate	case 2 composition	case 3 flow rate	case 3 composition
PP_1	0.995	1/0/0	3.296	1/0/0	2.974	$0.999/6 \times 10^{-5}/0$
PP_2	0.942	$4 \times 10^{-3}/0.996/9 \times 10^{-5}$	3.3	$1 \times 10^{-3}/0.994/4 \times 10^{-3}$	5.03	$5 \times 10^{-3}/0.994/3 \times 10^{-4}$
PP_3	8.06	$0/7 \times 10^{-3}/0.992$	3.403	$0/5 \times 10^{-3}/0.994$	1.998	$0/1 \times 10^{-4}/0.999$

Table 4. Models Size and Solver Times

	no. variables preprocessing phase	no. variables MINLP model	no. equations preprocessing phase	no. equations MINLP model	nonlinear elements preprocessing phase	nonlinear elements MINLP model	solution time[a] preprocessing phase	solution time[a] MINLP model
cases 1−3	2362	3879	1906	3327	5800	10863	3.1	2
case 2	2362	4808	1906	4469	5800	13455	3.1	4.6

[a] Times reported are CPU seconds on a Pentium III, 640 K, 500 MHz.

Figure 12. Reversible and adiabatic rectifying sections. (a) Reversible rectifying section. (b) Adiabatic rectifying section.

energy as in the reversible case is involved but located in the column top (see Figure 12b). Note that Q_C^{pinch} is the amount of energy continuously rejected to achieve the composition of the upper reversible exhausting pinch. This energy depends on the feed composition and on the volatility difference between its components. Instead, in the adiabatic separation, there is no energy involved between the feed stage and the saddle pinch point zone (see Figure 12b). The same holds for a reversible stripping section where a lower exhausting pinch point takes place.

Consider a ternary mixture; the reversible rectifying (stripping) profile points toward the simple vertex of the heaviest (lightest) component. This fact easily allows computing the reversible exhausting points that take place in a reversible column. The rectifying (stripping) binary pinch point composition can be calculated as the distillate (bottom) composition that would be achieved if the feed would have been separated through an indirect (direct) split. The reversible paths straightness is demonstrated next for the rectifying composition path but an analogous procedure can be done for a reversible stripping section. Note that this calculation procedure is extended straightforward to multicomponent mixtures. The upper (lower) reversible exhausting point is the point of the reversible composition profile where the heaviest (lightest) component is completely removed.

Consider a reversible rectifying section where the reversible separation task of a mixture containing n components is performed (see Figure 6a). Total mass balance and component mass balance can be formulated as follows:

$$L + D^{\text{rev}} = V \tag{A1}$$

$$Lx_i + D^{\text{rev}}x_i^{\text{rev}} = Vy_i \qquad i = 1, ..., n \tag{A2}$$

Equilibrium conditions must hold to avoid entropy production. The relationship between the vapor and liquid composition can be formulated for every component i:

$$K_i = \frac{y_i}{x_i} \tag{A3}$$

Assuming low-pressure conditions, the vapor phase can be modeled by Dalton law expressing the partial pressure p_i^{v} of a component i as a function of the total

pressure P of the vapor mixture. The liquid phase can be described by the Raoult law which provides an expression for the partial pressure p_i^{l} of component i over the liquid mixture as a function of its vapor pressure. If ideal behavior on the vapor phase is considered and the relative volatility of a component i with respect to another j is defined as follows:

$$\alpha_{ij} = \frac{x_i/y_i}{x_j/y_j} = \frac{P_i^o}{P_j^o} \tag{A4}$$

Assuming equilibrium conditions, expression (A3) can be rewritten as

$$K_i = \frac{\alpha_{ij}}{\displaystyle\sum_{k=1}^{n} x_k \alpha_{kj}} \tag{A5}$$

According to the reversible separation task, only the heaviest component n is completely removed from the top product ($d_n = 0$); then the following expression holds:

$$\frac{L}{V} = K_n = \frac{\alpha_{nj}}{\displaystyle\sum_{k=1}^{n} x_k \alpha_{kj}} \tag{A6}$$

Equation A2 can be rewritten as

$$d_i = (K_i - K_n)x_i \qquad i = 1, ..., n-1 \tag{A7}$$

Employing eqs A5 and A6, component i mole flow given by eq A7 can be expressed as

$$d_i = \frac{\alpha_{ij} - \alpha_{nj}}{\displaystyle\sum_{k=1}^{n} x_k \alpha_{kj}} x_i \qquad i = 1, ..., n-1 \tag{A8}$$

In an analogous way, the component l mole flow can be expressed as

$$d_l = \frac{\alpha_{lj} - \alpha_{nj}}{\displaystyle\sum_{k=1}^{n} x_k \alpha_{kj}} x_l \qquad \forall\, l \neq i \tag{A9}$$

Then, by expressing the quotient between (A8) and (A9),

$$\frac{x_i}{x_l} = \frac{d_i}{d_l} \frac{\alpha_{lj} - \alpha_{nj}}{\alpha_{ij} - \alpha_{nj}} \quad \text{(A10)}$$

Considering that the relative volatilities are constant, eq A10 demonstrates the straightness of the rectifying path because both quotients in the right-hand side of these expressions are constant.

Finally, note that the quotient between the top product flow of components i and l can be expressed as a function of the feed composition; then, expression (A10) can be written as

$$\frac{x_i}{x_l} = \frac{y_n^F x_i^F - y_i^F x_n^F}{y_n^F x_l^F - y_l^F x_n^F} \frac{\alpha_{lj} - \alpha_{nj}}{\alpha_{ij} - \alpha_{nj}} \quad \text{(A11)}$$

Appendix B: Ease of a Separation Index. Consider a ternary mixture with components A, B, and C, ordered in decreasing volatility. The ease of separation index (ESI)[11] is defined by the equation

$$\text{ESI} = \frac{\alpha_{AB}}{\alpha_B} = \frac{\alpha_A}{\alpha_B^2} \quad \text{(B1)}$$

where α_A is the relative volatility of the lightest component and α_B the relative volatility of the middle component of the mixture. Note that the heaviest component is considered as the reference component. When ESI is >1, distillation between A and B is easier compared to distillation between B and C and vice versa.

Appendix C: Efficiency Calculation. To compare different representations to approach reversibility conditions, a measure of the efficiency of the system has to be computed. We adopt the entropy produced in the system as a measure of its efficiency. The more efficient a system is, the lower irreversibilities it has and the lower entropy is generated.

Consider a sequence with a ncol adiabatic column from where p products emerge. The heat exchanged in the condenser and reboiler is carried out at constant temperature corresponding to the bubble point for the liquid mixture. The energy balance for the sequence and the entropy production rate σ_{seq} due to the existence of irreversibilities in the system are given by equations (C1) and (C2):

$$\Delta H_{\text{seq}} = \sum_{j=1}^{p} P \text{Hp}_j - F \text{Hf} = \sum_{j=1}^{\text{ncol}} (\text{Qh}_j + \text{Qc}_j) \quad \text{(C1)}$$

$$\sigma_{\text{seq}} = \sum_{j=1}^{p} P \text{Sp}_j - F \text{Sf} - \sum_{j=1}^{\text{ncol}} \left(\frac{\text{Qc}_j}{\text{Tc}_j} + \frac{\text{Qh}_j}{\text{Th}_j}\right) > 0 \quad \text{(C2)}$$

where Hp (Sp) and Hf (Sf) are the enthalpy (entropy) relative to the products and feed streams, respectively. The heat loads exchanged in a reboiler and in a condenser are Qh_j and Qc_j. Heat is only exchanged with the environment in the condensers at temperature Tc_j and in the reboilers at Th_j. Assume that any heat transfer irreversibility is excluded by defining those systems boundaries to be at temperature Tc_j and Th_j. Note that σ_{seq} accounts for all irreversibilities that take place in all stages of all columns, such as the mixing of streams at nonequilibrium temperature and composi-

tion. Since there are no other irreversibilities associated with a distillation system, σ_{seq} is the sum of the entropy production generated in each single unit of the sequence.

If reversibility conditions are assumed in every column, no entropy production takes place in the system. Then, the entropy change flow ΔS_{seq} between the products and the feed can be calculated by considering that the heat distribution functions along the stripping and rectifying sections, $\text{Qh}_j(T)$ and $\text{Qc}_j(T)$, respectively:

$$\Delta S_{\text{seq}} = \sum_{j=1}^{\text{ncol}} \left\{ \int_0^{\text{Qh}_j} \frac{d\text{Qh}_j(T)}{T} + \int_0^{\text{Qc}_j} \frac{d\text{Qc}_j(T)}{T} \right\} \quad \text{(C3)}$$

In the special case that each single unit of the sequence operates at minimum reflux conditions, the heat duties involved are the same as those in the reversible separation. Then, an expression based on the energy demand and its distribution along the reversible unit can be formulated:

$$\sigma_{\text{seq}} = \sum_{j=1}^{\text{ncol}} \left\{ \int_0^{\text{Qh}_j} \frac{d\text{Qh}_j(T_j)}{T_j} + \int_0^{\text{Qc}_j} \frac{d\text{Qc}_j(T_j)}{T_j} - \frac{\text{Qh}_j}{\text{Th}_j} - \frac{\text{Qc}_j}{\text{Tc}_j} \right\} \quad \text{(C4)}$$

A good measure for comparing the entropy generation in the RDS-based sequence is the summation of the quotient between the energy involved in each column extreme and the temperature in which the exchange occurs because ΔS_{seq} is constant. Then, only for comparing the efficiencies of distillation sequences with different energy distribution where the same final products are achieved, expression (C5) can be used to compute the entropy production:

$$\Delta \sigma_{\text{seq}} \approx - \sum_{j=1}^{\text{ncol}} \left\{ \frac{\text{Qc}_j}{\text{Tc}_j} + \frac{\text{Qh}_j}{\text{Th}_j} \right\} \quad \text{(C5)}$$

Nomenclature

bf_{nf}, n = binary variable denoting the existence of feed nf entering in tray n

bheat_n = binary variable denoting the existence of a reboiler in tray n

bp_{np}, n = binary variable denoting the existence of product np leaving tray n

$\hat{f}_{n,i}^L$ = fugacity of component i in the liquid leaving tray n

$\hat{f}_{n,i}^V$ = fugacity of component i in the vapor leaving tray n

F_{nf}, n = flow rate of feed nf entering in tray n (mol/s)

F_0 = flow rate of initial feed (mol/s)

Fmax_{nf} = upper bound for the flow rate of feed nf (mol/sec)

hf_{nf} = enthalpy of feed nf (kJ/mol)

hf_0 = enthalpy of initial feed (kJ/mol)

hl_n = enthalpy of liquid leaving tray n (kJ/mol)

hP_m = enthalpy of final product m (kJ/mol)

hv_n = enthalpy of vapor leaving tray n (kJ/mol)

hpl_j = enthalpy of liquid flow contributing to product in integration j (kJ/s)

hpv_j = enthalpy of vapor flow contributing to product in integration j (kJ/s)

L_n = flow rate of liquid leaving tray n (mol/s)

P_n = total pressure in tray n (bar)

PL_n = flow rate of liquid product leaving tray n (mol/s)

PP_m = flow rate of final product m (mol/s)

ppl_j = liquid flow contributing to final product in integration j (mol/s)

ppv_j = vapor flow contributing to final product in integration j (mol/s)

PV_n = flow rate of vapor product leaving tray n (mol/s)

Q_n = energy demand on tray n (kJ/s)

$Qctot_j$ = condenser heat duty (kJ/s)

$Qhtot_j$ = reboiler heat duty (kJ/s)

Qmax = upper bound for the energy exchanged in the condenser (kJ/s)

$Q_{phase\ j}$ = energy exchanged in integration j (kJ/s)

T_n = temperature of tray n (K)

V_n = flow rate of vapor leaving tray n

$x_{n,i}$ = liquid composition of component i leaving tray n (mole fraction)

$y_{n,i}$ = vapor composition of component i leaving tray n (mole fraction)

zf_{nf},i = composition of component i in feed nf (mole fraction)

zf_0 = initial feed composition (mole fraction)

$zP_{m,i}$ = composition of component i in the final product m (mole fraction)

$zpl_{j,i}$ = composition of component i in the liquid flow contributing to product in integration j (mole fraction)

$zpv_{j,i}$ = composition of component i in the vapor flow contributing to product in integration j (mole fraction)

Literature Cited

(1) Bruggemann, S.; Marquardt, W. *Shortcut Methods for Nonideal Multicomponent Distillation: Providing Initials and Bounds for Rigorous Optimization.* Internal Report, May 20, 2001.

(2) Yeomans, H.; Grossmann, I. E. Disjunctive Programming Models for the Optimal Design of Distillation Columns and Separation Sequences. *Ind. Eng. Chem. Res.* **2000**, *39*, 1637.

(3) Yeomans, H.; Grossmann, I. E. Optimal Design of Complex Distillation Columns Using Rigorous Tray-by-Tray Disjunctive Programming Models. *Ind. Eng. Chem. Res.* **2000**, *39*, 4326.

(4) Barttfeld, M.; Aguirre, P. A.; Grossmann, E. I. Alternative Representations and Formulations for the Economic Optimization of Multicomponent. *Comput. Chem. Eng.* **2003**, in press.

(5) Fonyó, Z. Thermodynamic Analysis of Rectification I. Reversible Model of Rectification. *Int. Chem. Eng.* **1974**, *14* (1), 18.

(6) Koehler, J.; Aguirre, P. A.; Blass, E. Evolutionary Thermodynamic Synthesis of Zeotropic Distillation sequences. *Gas Sep. Purif.* **1992**, *6* (3), 153.

(7) Stilchmair, J. G.; Fair, J. R. *Distillation, Principles and Practice*; Wiley-VCH: New York, 1998.

(8) Kaibel, G.; Blass, E.; Koehler, J. Thermodynamics—Guideline for the Development of Distillation Columns Arrangements. *Gas Sep. Purif.* **1990**, 4 June, 109.

(9) Barttfeld, M.; Aguirre, P. A. Optimal Synthesis of Distillation Processes. Part I. Preprocessing Phase for Zeotropic Mixtures. *Ind. Eng. Chem. Res.* **2002**, *41*, 5298.

(10) Aguirre, P. A.; Corsano, G.; Barttfeld, M. Un Método Híbrido para la Síntesis Óptima de Procesos de Destilación Multicomponente. *CIT (Información Tecnológica)* **2001**, *12* (1), 119.

(11) Tedder D. W.; Rudd D. F. Parametric Studies in Industrial Distillations: Part 1. Design Comparisons. *AIChE J.* **1978**, *24*, 303.

(12) Reid, R. C.; Prausnitz, M. P.; Poling, B. E. *The Properties of Gases and Liquids*; McGraw-Hill: New York, 1987.

(13) Bauer, M. H.; Stichlmair, J. Design and Economic Optimization of Azeotropic Distillation Processes Using Mixed-Integer Nonlinear Programming. *Comput. Chem. Eng.* **1998**, *22* (9), 1271.

(14) Brooke, A.; Kendrick, D.; Meeraus, A.; Raman, R. *GAMS, A User Guide*; 1998.

(15) Agrawal, R.; Fidkowski, Z. T. Are Thermally Coupled Distillation Columns Always Thermodynamically More Efficient for Ternary Distillations? *Ind. Eng. Chem. Res.* **1998**, *37*, 3444.

(16) Agrawal, R.; Fidkowski, Z. T. Thermodynamically Efficient Systems for Ternary Distillations. *Ind. Eng. Chem. Res.* **1999**, *38*, 2065.